Efficient Visible-Light-Induced Photocatalytic Activity of a 3D-Ordered Titania Hybrid Photocatalyst with a Core/Shell Structure of Dye-Containing Polymer/Titania

ARTICLE *in* THE JOURNAL OF PHYSICAL CHEMISTRY C · SEPTEMBER 2008

Impact Factor: 4.77 · DOI: 10.1021/jp8055152

5 AUTHORS, INCLUDING:

Yuanzhi Li
Wuhan University of Technology
60 PUBLICATIONS **1,989** CITATIONS
SEE PROFILE

X. L. Hu
Harbin Institute of Technology
76 PUBLICATIONS **1,420** CITATIONS
SEE PROFILE

Xiujian Zhao
Wuhan University of Technology
461 PUBLICATIONS **7,347** CITATIONS
SEE PROFILE

Efficient Visible-Light-Induced Photocatalytic Activity of a 3D-Ordered Titania Hybrid Photocatalyst with a Core/Shell Structure of Dye-Containing Polymer/Titania

Yuanzhi Li,*,† Hua Zhang,† Xuelei Hu,‡ Xiujian Zhao,† and Min Han§

Key Laboratory of Silicate Materials Science and Engineering, Wuhan University of Technology, Ministry of Education, 122 Luoshi Road, Wuhan, 430070, People's Republic of China, State Key Laboratory of High Performance Ceramics and Superfine Microstructure, School of Chemical Engineering and Pharmacy, Wuhan Institute of Technology, 693 Xiongchu Road, Wuhan, 430073, People's Republic of China, and School of Chemistry and Chemical Engineering, Nanjing University, Nanjing, 210093, People's Republic of China

Received: June 23, 2008; Revised Manuscript Received: July 04, 2008

Photostable 3D-ordered titania hybrid photocatalyst with the core/shell structure of dye-containing polymer/titania was prepared by layer-by-layer coating of adsorption and hydrolysis of $Ti(OBu)_4$ on fluorescent polystyrene microspheres (YG), in which a sensitized dye of fluorescein isothiocyanate with a strong absorption in the visible light region of 400−500 nm is fixed. Photocatalytic tests show that the nanostructured titania hybrid photocatalyst exhibited efficient and stable photocatalytic activity for the photodegradation of crystal violet (CV) under visible light irradiation. The titania hybrid photocatalyst was characterized by UV−visible spectroscopy, SEM, TEM, XRD, photoluminescence (PL), time-resolved fluorescence, and electrochemical measurement. The characterization results show that the dye in YG spheres acts as a sensitizer for titania. By absorbing a visible photon it is promoted to an excited electronic state YG*, from which an electron can be injected into the conduction band of titania on the interface of YG spheres and titania shell. The electron subsequently induces the generation of active oxygen species, which result in the degradation of CV. The produced YG^+ radical cation can react with CV to realize the recycling of the photosensitized dye. The photodegradation of CV on TiO_2−YG undergoes two competitive mechanisms: *N*-demethylation and destruction of the conjugated structure. The *N*-demethylation process predominates during the initial irradiation period. Later, the process of ring rupture is significant. It is evidenced that the *N*-didemethylated intermediate and the *N*-tridemethylated intermediate of CV undergo a direct cleavage of their conjugated structures.

Introduction

Nanostructured titania as a cheap, nontoxic, efficient photocatalyst is one of the most popular and promising materials for the detoxification of air and water pollutants. However, it is activated only under UV light irradiation because of its large band gap (3.2 eV for anatase, and 3.0 eV for rutile). But solar spectra contain only 5% UV light; therefore, 95% of the solar photons are useless for TiO_2 photocatalyst, which greatly limits its practical application in environmental decontamination. Therefore, it is crucial and a great challenge to explore efficient visible-light-induced photocatalysts by the modification of titania. To achieve such goal, diverse efforts have been made during recent years to shift the response of TiO_2 into the visible region. These works included the following: (1) doping TiO_2 with various transitions metals;[1−3] (2) doping TiO_2 with nonmetal atoms such as N, C, S, I, etc.;[1,4−9] and (3) sensitizing titania with colorful inorganic materials such as I_2[10] and silver halide.[11] Because of the relative low absorption coefficient of the doped and sensitized titania in the visible range, it is highly desirable to explore a new material system that can effectively utilize visible light.

Organic dye has a high absorption coefficient to the visible light. When anchored on the surface of titania, it efficiently absorbs visible light, and the photoinduced electron can transfer from the excited dye to the conduction band of titania. This dye sensitization has been extensively studied for titania-based solar cells. However, it seldom has been used in constituting a photocatalyst for detoxification of wastewater due to the instability and self-photodegradation of dye with illumination under aerobic condition.[12] Bae et al.[13] reported that ruthenium bipyridyl complexes can be used to sensitize TO_2 for organic detoxification. However, the ruthenium bipyridyl complexes are unstable under visible irradiation, and readily experience self-photodegradation. It was found that some phthalocyanine derivates are stable in dye sensitization photocatalysis.[14] But crystalline anatase and rutile are necessary for constituting phthalocyanine/TiO_2 photocatalyst, while amorphous TiO_2 was reported to be photoinactive.[15] Recently, Chen et al.[16] prepared a hybrid photocatalyst of 2,9,16,23-tetracarboxyl phthalocyanine (TcPc)/amorphous TiO_2 and found that it exhibited good photocatalytic activity under visible light irradiation. However, typical preparation for phthalocyanine/TiO_2 photocatalyst always involved an uncharitable solvent such as sulfuric acid, which is destructive to TiO_2 and possibly leads to some unpredictable changes to the physicochemical properties of TiO_2.[16] Another involved problem for the dye-sensitized photocatalysts is difficulty in the separation of the sensitized dye from wastewater because of its solubility in water, which is dependent on the pH value.

It is well-known that anchoring dye on a textile or fixing a dye molecule in a polymer by copolymerization can greatly improve the photostability of the dye, and make the dye

* Corresponding author.
† Key Laboratory of Silicate Materials Science and Engineering, Wuhan University of Technology.
‡ School of Chemical Engineering and Pharmacy, Wuhan Institute of Technology.
§ School of Chemistry and Chemical Engineering, Nanjing University.

10.1021/jp8055152 CCC: $40.75
Published on Web 09/03/2008

insoluble in water. Herein, we developed a facile approach of preparing a photostable 3D-ordered titania hybrid photocatalyst with a core/shell structure of dye-containing polymer/titania, and found that it exhibited efficient photocatalytic activity under irradiation of visible light.

Experimental Section

Materials. Monodispersed polystyrene spheres (2.62% solid latex, diameter 202 nm, standard deviation 10 nm, denoted as PS spheres) and monodispersed fluorescent polystyrene microspheres (Fluoresbrite plain YG microsphere, 2.72% solid latex, diameter 200 nm, standard deviation 12 nm, denoted as YG spheres) were bought from Polysciences. The latter latex is modified with fluorescein isothiocyanate.[17] Titanium butoxide ($Ti(OBu)_4$) was purchased from Shanghai Aisi Chemical Reagent Co. Crystal violet and hydrochloric acid were purchased from Shanghai Chemical Co.

Fabrication of Ordered YG Spheres/TiO_2 Hybrid Films. Ordered latex films of YG spheres were fabricated on glass slides (1.9×1.3 cm^2) by our previously developed sonication-assisted casting.[17] Subsequent titania casting was conducted as follows. Hydrochloric acid (25 μL, 1.5 mol/L) and 50 μL of deionized water were mixed with 5 mL of ethanol, and then 25 μL of neat titanium(IV) butoxide was added under magnetic stirring. Fifty microliters of the mixture was spread uniformly on the whole area of the 3D-ordered latex film and allowed to penetrate into the film interior. After the solvent was evaporated, the film was dried at ambient temperature, then transferred to an oven with controlled humidity (70%) and temperature (50 °C) for 5 min. The adsorbed titania precursor was completely hydrolyzed to amorphous titania. The penetration process was repeated 5 times. The film was covered by another glass slide and placed in 0.08 mol/L dilute hydrochloric acid in a small bottle. The bottle was kept in a container at 70 °C for 48 h. The obtained sample was denoted as TiO_2−YG.

Characterization. Scanning electron microscopy (SEM) images were obtained by using a Hitachi S-5200 scanning electron microscope. Transmission electron microscopy (TEM) images were obtained by using a JEM-100CX electron microscope. For preparing the TEM grid with the sample, the sample was scratched from the glass substrate and then dispersed in ethanol. X-ray diffraction (XRD) patterns were obtained on a Rigaku D/Max-IIIA X-ray diffractometer, using Cu Kα radiation. UV−vis absorption spectra were recorded on a UV-240 UV−visible spectrophotometer. Photoluminescence spectra were recorded at room temperature on a SHIMADZU RF-5301 PC spectrometer, using 440 nm excitation light. Fluorescence lifetimes were determined with a FLS920 spectrometer, which permitted automatic fitting of the data. Cyclic voltammetric measurement of the samples was carried out by using a standard three-electrode cell with distilled water as the electrolyte, Pt wire as the counter electrode, a saturated Hg_2Cl_2/Hg reference electrode as the reference electrode, and a Pt plate as the working electrode on an electrochemical analyzer (CHI750). Before the measurement, the electrolyte was purged by pure N_2. For measuring the potential of YG, the YG thin film was deposited on a Pt plate electrode by using the YG solution in toluene.

Photocatalytic Activity. Photodegradation of crystal violet was chosen to evaluate the photocatalytic activity of the samples. First, 20 μL of 1.0 mmol/L crystal violet in ethanol was dropped on the film. After being dried at room temperature in the dark, the film was fixed on a shelf under a 500 W Xe lamp, and the lamp was turned on. A UV cut-filter, which can filter out UV light with wavelengths below 420 or 520 nm, was placed between the film and the Xe lamp. After irradiation, the film was immersed in 6 mL of ethanol to dissolve the unreacted dye, then was washed with 1 mL of ethanol. The dye concentration was determined by measuring the UV−vis absorbance of the washing.

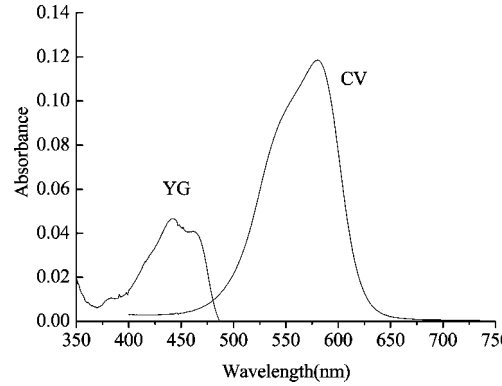

Figure 1. Absorption spectra of YG and CV.

The durability experiment of the film was carried out according to the following procedure. Twenty microliters of 1.0 mmol/L crystal violet in ethanol was dropped on the film. After being dried at room temperature in the dark, the film was irradiated for 40 min under the illumination of a Xe lamp. After irradiation, the film was immersed in 6 mL of ethanol to dissolve the unreacted dye, then was washed with 1 mL of ethanol. The film was recycled for the next photocatalytic test.

Results and Discussion

Characterization. In this work, we aimed at designing efficient visible-light-induced photocatalyst. So, we selected fluorescein isothiocyanate in YG spheres as the sensitized dye because the dye has a strong absorption in the range of 400 to 500 nm as shown in Figure 1. A titania-coated fluorescent microsphere was prepared by layer-by-layer coating of adsorption and hydrolysis as described in the Experimental Section. Figure 2 shows SEM images of a film of YG spheres before and after titania coating. The top surface given in Figure 2a is composed of a closely packed, hexagonal array of latex spheres with a diameter of 200 nm and a smooth surface. After titania coating, the ordered structure remains unchanged except for the sphere surface becoming rugged due to the formation of the titania shell on the latex spheres. The diameter of the latex sphere coated with titania nanoparticles increases to 209 nm, indicating that the titania shell with a thickness of 4.5 nm is formed on the latex sphere. A cross-section SEM image of Figure 2c shows that 13 layers of titania coated latex spheres are closely packed along the direction perpendicular to the surface. As shown in Figure 2d, the TEM image of titania coated latex spheres indicates that the titania shell with an average thickness of 4.5 nm is formed on the latex spheres. After dissolving YG spheres in TiO_2−YG with toluene, the unsupported titania shell was obtained (Figure 2e). The titania shell is composed of titania nanoparticles with sizes of 3−10 nm, among which there are pores with sizes of 2−6 nm. The porous structure of the titania shell is beneficial for the diffusion of both reactants and products, which is helpful for improving photocatalytic efficiency. Figure 3 shows the XRD pattern of the film of TiO_2−YG spheres. As can be seen form Figure 3, titania coated on YG spheres is amorphous.

Photoluminescence and Charge Transferring. Figure 4 presents the photoluminescence (PL) spectra of a film of YG

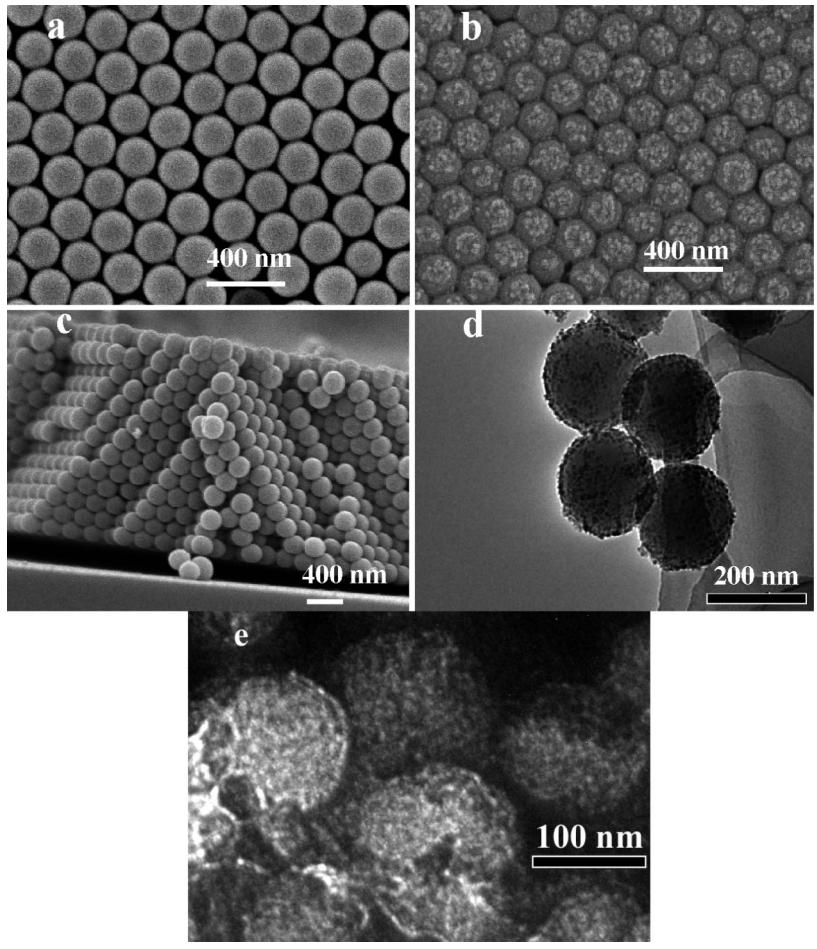

Figure 2. Morphology of the film of TiO_2−YG spheres: SEM images (top view) of the film of YG spheres (a) and TiO_2−YG spheres (b), SEM image (cross-section view) of the film of TiO_2−YG spheres (c), TEM image of TiO_2−YG spheres (d), TEM image of the TiO_2 shell obtained by dissolving the YG spheres of TiO_2−YG spheres with toluene (e).

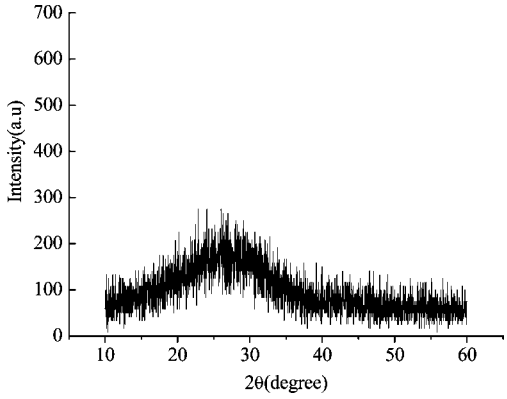

Figure 3. XRD pattern of the film of TiO_2−YG spheres.

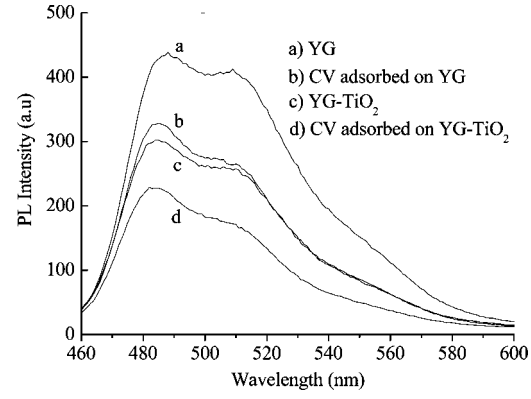

Figure 4. The room temperature photoluminescence spectra with excitation at 440 nm for the photocatalysts.

spheres before and after coating with titania. The film of YG spheres has two strong PL emission peaks at 512 and 483 nm resulting from fluorescein isothiocyanate. In contrast, coating titania on YG spheres leads to a great decrease of PL intensity, which is ascribed to the injection of the photoexcited electron from the excited dye to the conduction band of titania.[18] The redox potential of YG^+/YG was measured with the cyclic voltammetric method (platinum and saturated Hg_2Cl_2/Hg as working and reference electrodes, respectively). The obtained redox potential of YG^+/YG is 1.1 V (vs Hg_2Cl_2/Hg). As the maximum absorption of YG is 442 nm (2.80 eV), the potential of photoexcited YG* is −1.46 eV vs NHE, which is less than the energy level of the conduction band of TiO_2 (around −0.1 eV vs NHE).[19] This makes the occurrence of the interfacial electron injection thermodynamically possible.

As shown in Figure 4, adsorption of CV on YG spheres leads to a decrease of PL intensity. A similar phenomenon was observed for adsorption of CV on TiO_2−YG spheres. These results suggest that there is charge transferring between CV and YG. The measured redox potential of CV^+/CV is 0.2 V (vs Hg_2Cl_2/Hg). Considering that the maximum absorption of CV is 580 nm (2.13 eV), the higher potential of photoexcited YG* (−1.46 eV vs NHE) than that of CV* (−1.69 eV vs NHE) excludes the possibility of the injection of the photogenerated electron from YG* to CV. The higher potential of YG^+/YG

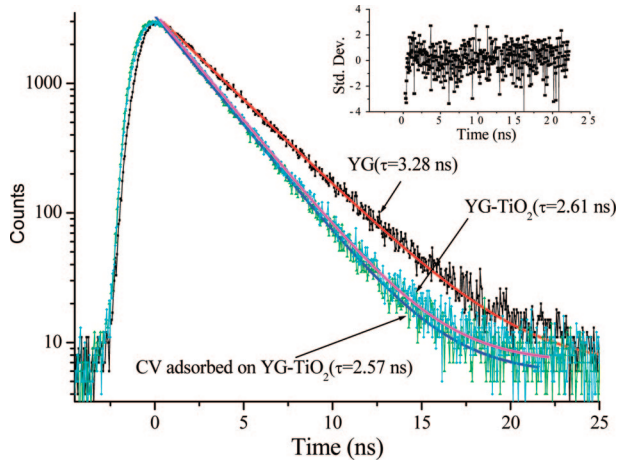

Figure 5. Fluorescence emission decay for the samples (the inset is the curve of standard deviation). The excitation wavelength was 410 nm, and the fluorescence emission was recorded at 483 nm.

SCHEME 1: Schematic Illustration of the Mechanism for the Photodegradation of CV on TiO_2−YG Spheres

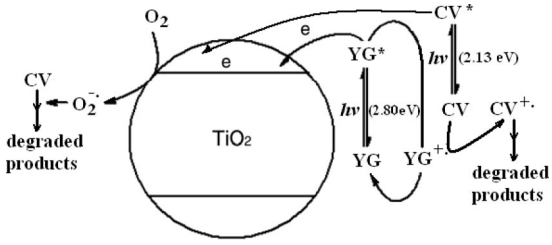

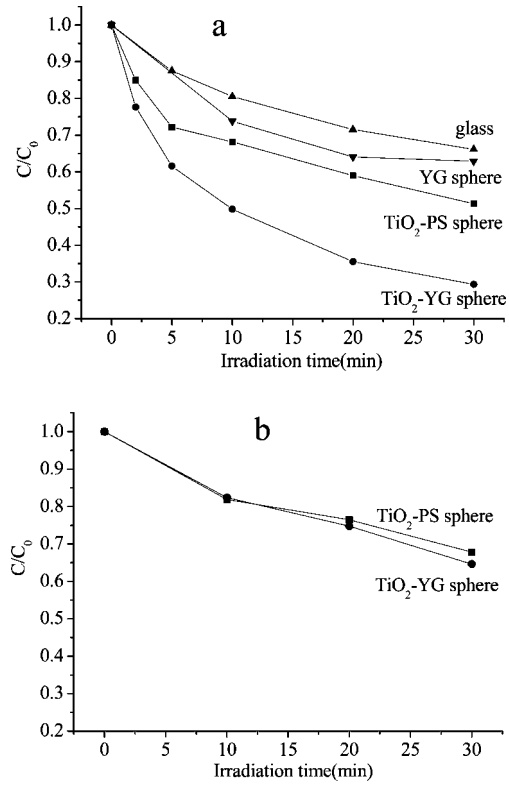

Figure 6. Decreases in the dye concentration and with solar light under visible light irradiation of $\lambda > 420$ nm (a) and $\lambda > 520$ nm (b).

than CV^+/CV indicates that the photogenerated YG^+ radical cation could react with CV as follows on the interface of YG spheres and titania to realize charge transfer between CV and YG (Scheme 1):

$$CV + h\nu \rightarrow CV^*$$

Therefore, the photoluminescence quenching of YG by CV is most probably due to the charge transfer between CV and YG^+.

Fluorescence Lifetime. To study the charge transferring process in the above samples, time-resolved fluorescence measurements were carried out. Figure 5 shows the fluorescence decay of YG, TiO_2−YG, and CV adsorbed on TiO_2−YG exciting at 440 nm. The fluorescence decay of YG could be fitted well with a single-exponential curve with a fluorescence lifetime of 3.28 ns. Coating TiO_2 on YG spheres leads to faster fluorescence decay, which also could be described by single-exponential kinetics. Its corresponding fluorescence lifetime is 2.61 ns. The decrease in lifetimes is attributed to interfacial electron transfer from the excited dye (YG*) to the conduction band of titania.[18,20] According to the equation $k_{ET} = 1/\tau - 1/\tau_o$[18b,20] ($k_{ET}$ denotes the rate constant of electron transfer; τ and τ_o are the fluorescence lifetimes of TiO_2−YG and YG, respectively), we can calculate that $k_{ET} = 7.8 \times 10^7\ s^{-1}$. As shown in Figure 5, TiO_2−YG with absorbed CV exhibits almost the same fluorescence decay curve as TiO_2−YG. This observation indicates that there is no injection of the photogenerated electron from YG* to CV, which is in good agreement to the result obtained by the above electrochemical measurement and photoluminescence.

Photocatalytic Degradation of CV. Dye effluents from textile industries are becoming a serious environment problem because of their unacceptable color, high chemical oxygen demand content, and resistance to chemical, photochemical, and biological degradation. Effective utilization of solar light to degrade organic wastes and spent dyes in the presence of titania is expected to provide an attractive approach for environmental remediation.[21] We chose photodegradation of crystal violet dye with visible light to evaluate the photocatalytic activity of the films. Previously, we reported that the photocatalytic activity of 3D-ordered titania spheres can be enhanced by the stop band effect of the photonic crystal and multiple scattering, which are dependent on the diameter of the spheres.[22] To avoid such effects, we prepared a 3D-ordered polystyrene latex sphere coated with titania (denoted as TiO_2−PS) with almost the same diameter (202 nm) as the reference sample for comparison by a procedure similar to that of TiO_2−YG. Figure 6a shows the time course of the decrease in the dye concentration with irradiation of the visible light ($\lambda > 420$ nm). As shown in Figure 6a, CV adsorbed on a glass slide is slowly photodegraded with time. After irradiation for 30 min, 34% of CV is photodegraded. As glass is photocatalytically inactive, the photodegradation of CV undergoes a self-photosensitive pathway as follows:

$$CV^* + O_2 \rightarrow \rightarrow \text{degraded products}$$

$$CV + h\nu \rightarrow CV^*$$

Compared to glass, the film of TiO_2−PS clearly accelerates the photodegradation process, in which 49% of CV is photodegraded after irradiation for 30 min. This photocatalytic enhancement is attributed to the self-photodegradation of CV through the photocatalytic pathway of CV photosensitized TiO_2[23] (Scheme 1) on the titania shell of TiO_2−PS. CV absorbing a visible photon is promoted to an excited electronic state CV*, from which an electron can be transferred into the conduction band of titania:

$$CV + h\nu \rightarrow CV^*$$

$$CV^* + TiO_2 \rightarrow CV^+ + TiO_2(e^-)$$

Once the electron reaches the TiO_2 conduction band, it subsequently induces the generation of active oxygen species, which result in the self-degradation of CV.

Compared to TiO_2−PS, TiO_2−YG shows much enhanced photocatalytic activity with 71% of CV photodegradation after irradiation for 30 min. Clearly, apart from the self-photodegradation of CV through the photocatalytic pathway of CV-photosensitized TiO_2, there is another kind of photocatalytic pathway to account for the enhanced photocatalytic activity for TiO_2−YG. As shown in Figure 1, the dye in TiO_2−YG has a strong absorption in the range of 400−500 nm. The much enhanced photocatalytic activity of TiO_2−YG compared to TiO_2−PS suggests that the photodegradation of CV undergoes a photocatalytic pathway of YG-photosensitized TiO_2 as illustrated in Scheme 1. The dye in YG spheres absorbing a visible photon is promoted to an excited electronic state YG*, from which an electron can be transferred into the conduction band of titania on the interface of YG spheres and the titania shell:

$$YG + h\nu \rightarrow YG^*$$

$$YG^* + TiO_2 \rightarrow YG^+ + TiO_2(e^-)$$

The photogenerated electron in the TiO_2 conduction band subsequently induces the generation of active oxygen species, which result in the degradation of CV.

As concluded in the PL discussion, there is charge transfer between photoexcited YG* and CV. To confirm whether photoexcited YG* initiates photodegradation of CV, we tested the photodegradation of CV on the film of YG spheres. As shown in Figure 6a, compared to photodegradation of CV on glass (34% of CV photodegradation after irradiation for 30 min), YG spheres just exhibit a slightly higher photocatalytic activity with 37% of CV photodegradation after irradiation for 30 min. The surface area of the film of YG spheres with a diameter of 200 nm on a glass slide (1.9×1.3 cm^2) is calculated to be 3.9×10^{-2} m^2, which is 158 times larger than that of the glass slide (2.47×10^{-4} m^2). The similar photocatalytic activity of the film of YG spheres and the glass slide suggests that the photodegradation of CV through the photosensitive pathway is generally independent of the surface area of substrate in our case. On the other hand, the TiO_2−YG photocatalyst has almost the same surface area as TiO_2−PS. Therefore, the photodegradation of CV through the photosensitive pathway makes the same contribution to the total photodegradation of CV on both TiO_2−YG and TiO_2−PS. These results indicate that the enhanced photocatalytic activity of TiO_2−YG compared to TiO_2−PS is mainly due to photocatalytic degradation initiated by YG-sensitized TiO_2. The CV degradation through the photosensitive oxidation initiated by YG excitation makes very little contribution to the enhanced photocatalytic activity, probably due to the fastest recombination of photogenerated hole−electron pair in YG* in the absence of TiO_2 as shown in Figure 4.

To further confirm this photosensitization effect of YG photosensitized TiO_2, we tested the photocatalytic activity of the samples under the irradiation of visible light with higher wavelength ($\lambda > 520$ nm). As shown in Figure 6b, in contrast to the much higher photocatalytic activity of TiO_2−YG than that of TiO_2−PS under irradiation of $\lambda > 420$ nm, the former photocatalyst has almost the same photocatalytic activity as the latter under irradiation of $\lambda > 520$ nm. As the dye in YG spheres has no absorption above $\lambda > 520$ nm, titania could not be photosensitized by the dye, which results in the absence of photosensitization of titania by the dye. There just exists the photosensitization effect of CV photosensitized TiO_2 both on TiO_2−YG and on TiO_2−PS because the maximum absorptions of CV are centered at 580 nm (Figure 1), which leads to their similar photocatalytic activity under irradiation of $\lambda > 520$ nm.

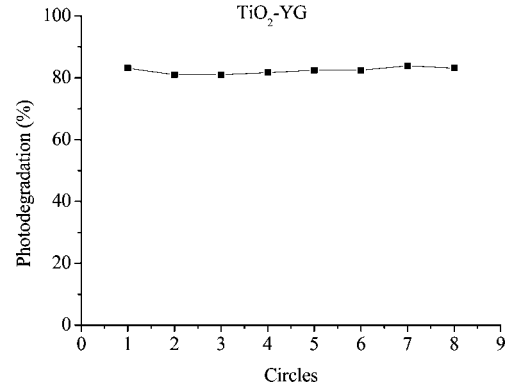

Figure 7. The durability of the TiO_2−YG sphere photocatalyst for the photodegradation of CV under the illumination of a Xe lamp.

Figure 7 shows the durability of the TiO_2−YG photocatalyst for the photodegradation of CV under the illumination of a Xe lamp. The photocatalytic activity of TiO_2−YG remains unchanged after eight successive cycles. The result demonstrates that TiO_2−YG is an effective and stable photocatalyst, and the photosensitization effect of YG-photosensitized TiO_2 on TiO_2−YG keeps working even if operating for a long period of time.

The stability of TiO_2−YG under the illumination of a Xe lamp for a long period of time suggests that the produced YG^+ radical cation could not itself lead to degradation. The question is how does the photosensitized dye realize its recycling of YG^+ to YG. As discussed above, the produced YG^+ radical cation can react with CV on the interface of YG spheres and titania to realize the recycling of the photosensitized dye (Scheme 1). The produced CV^+ radical cation moves to the surface of the titania shell, and reacts with adsorbed active oxygen species, which results in the degradation of CV.

The Mechanism of Photodegradation. It has been reported that CV exhibits two main mechanisms of photodegradation:[24,25] One mechanism involves *N*-demethylation while the aromatic structure of the molecule is preserved. In this process, the N atom of CV is attacked by the active oxygen species, which results in the removal of the terminal methyl group. The consecutive removal of all six terminal methyl groups finally gives rise to a complete transformation of CV into fuchsine basic (FB), with an adsorption maximum displacement from 590 to 540 nm. The *N*-demethylated intermediate species include mono-, di-, tri-, tetra-, and pentademethylated CV species, the adsorption maximums of which are 581 (*N*,*N*-dimethyl-*N*′,*N*′-dimethyl-*N*″-methylpararosaniline), 579.8 (*N*,*N*-dimethyl-*N*′,*N*′-dimethylpararosaniline) or 573.7 (*N*,*N*-dimethyl-*N*′-methyl-*N*″-methylpararosaniline), 570 (*N*,*N*-dimethyl-*N*′-methylpararosaniline) or 566.3 (*N*-methyl-*N*′-methyl-*N*″-methylpararosaniline), 561.5 (*N*-dimethyl-*N*′-methylpararosaniline) or 566.3 (*N*,*N*-dimethylpararosaniline), and 554.1 nm (*N*-methylpararosaniline), respectively.[26] The other mechanism involves the destruction of the conjugation structure. In this case, the conjugated structure of CV is attacked by active oxygen species, leading to the rupture of the conjugated structure and instant bleaching of the aromatic dyes.

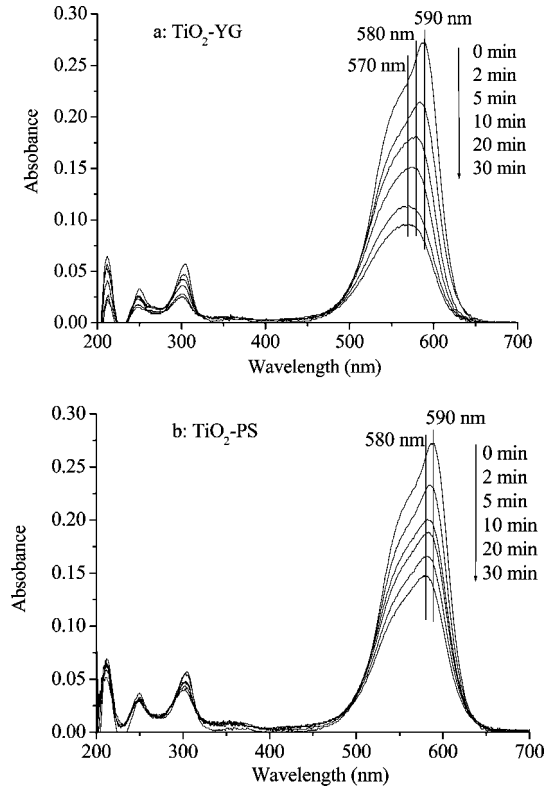

Figure 8. Temporal UV−visible absorption spectral changes for the photodegradation of CV on TiO_2−YG (a) and TiO_2−PS (b) as a function of irradiation time (λ > 420 nm).

Figure 8a shows the temporal evolution of absorption spectra of CV on TiO_2−YG under visible light irradiation (>420 nm). With increasing irradiation time from 0 to 5 to 20 min, the maximum absorption peak decreases with hypsochromic shift from 590 to 580 to 570 nm. The hypsochromic shift is due to consecutive *N*-demethylation reactions, corresponding to the removal of two and three terminal methyl groups,[26] respectively. Further increasing irradiation time does not lead to the appearance of additional hypsochromic shift as well as new absorption bands even in the ultraviolet range (λ > 200 nm). The observation suggests a direct cleavage of the whole conjugated chromophore structure of the *N*-tridemethylated intermediate and no appearance of tetra-, penta-, and hexademethylated CV species.

As shown in Figure 8b, a hypsochromic shift of 10 nm was observed in the initial 5 min for the photodegradation of CV on TiO_2−PS, indicating the formation of *N*-didemethylated intermediates.[26] With increasing irradiation time from 5 to 30 min, no hypsochromic shift is observed. However, there is rapid absorbance decay. The observation suggests a direct cleavage of the whole conjugated structure of the *N*-didemethylated intermediate and no appearance of tri-, tetra-, penta-, and hexademethylated CV species.

From the above results we can see that the photodegradation of CV on both TiO_2−YG and TiO_2−PS undergoes two competitive mechanisms: *N*-demethylation and destruction of the conjugated structure. The *N*-demethylation process predominates during the initial irradiation period. Later, the process of ring rupture is significant. It is evidenced that the *N*-didemethylated intermediate and the *N*-tridemethylated intermediate of CV undergo a direct cleavage of their conjugated structures.

Designing a 3D-ordered titania hybrid photocatalyst of dye-containing polymer/TiO_2 with core/shell structure has several advantages. First, the fixation of a sensitized dye in polymer is favorable for the improvement of the stability of the dye and making the dye insoluble in wastewater, while its high absorption coefficient of visible light can be fully used in dye-sensitized titania hybrid photocatalysts. Second, the YG sphere as a core absorbs visible light, the photogenerated electron transfers to the conduction band of the outside porous titania shell, where photodegradation of dye takes place. This nanostructure significantly decreases the diffusion length of reactants and products, which is beneficial for the improvement of photocatalytic activity. Finally, the strong UV absorption of titania in the outside shell can prevent UV irradiation on the dye-containing polymer in the inner core and thus further improve its photostability for UV irradiation while the high efficient photocatalytic activity of titania under UV irradiation is kept. It should be noted that the efficiency of the visible-light-induced photocatalytic activity depends on the interaction of the sensitized dye and titania on the interface of dye-containing polymer and titania. It is expected that the larger the interface is, the higher the photocatalytic activity. In the present case, the surface area of YG spheres with a diameter of 200 nm is calculated to be 28 m^2/g. It is anticipated that increasing the surface area of YG spheres by decreasing their diameter would lead to the enhancement of photocatalytic activity.

Conclusion

In summary, a facile approach was developed to prepare a photostable 3D-ordered titania hybrid photocatalyst with a core/shell structure of dye-containing polymer/titania. The nanostructured titania hybrid photocatalyst exhibited stable and efficient photocatalytic activity for the photodegradation of CV under visible light irradiation. The efficient visible-light-induced photocatalytic activity is attributed to the photosensitization effect of titania sensitized by the dye in YG spheres. The dye absorbing a visible photon is promoted to an excited electronic state YG*, from which an electron can be transferred into the conduction band of titania on the interface of YG spheres and the titania shell. Once the electron reaches the TiO_2 conduction band, it subsequently induces the generation of active oxygen species, which result in the degradation of CV. The photogenerated YG^+ radical cation can react with CV to realize the recycling of the photosensitized dye. Our approach provided a novel strategy for designing stable and efficient visible-light-induced photocatalysts. It is hopeful for our approach to be extended to design a stable and highly efficient solar cell.

Acknowledgment. This work was supported by the National Science Foundation (20743001), the Talented Young Scientist Foundation (2007ABB034) of Hubei Province, China, the Program for New Teacher from Ministry of Education (20070497003), and the Opening Project of State Key Laboratory of High Performance Ceramics and Superfine Microstructure (SKL200704SIC).

References and Notes

(1) Chen, X. B.; Mao, S. S. *Chem. Rev.* **2007**, *107*, 2891.

(2) Kisch, H.; Zang, L.; Lange, C.; Maier, W. F.; Antonius, C.; Meissner, D. *Angew. Chem., Int. Ed.* **1998**, *37*, 3034.

(3) Bosc, F.; Ayral, A.; Keller, N.; Keller, V. *Appl. Catal., B* **2007**, *69* (3−4), 133.

(4) Asahi, R.; Ohwaki, T.; Aoki, K.; Taga, Y. *Science* **2001**, *293*, 269.

(5) Livraghi, S.; Paganini, M. C.; Giamello, E.; Selloni, A.; Di Valentin, C.; Pacchioni, G. *J. Am. Chem. Soc.* **2006**, *128*, 15666.

(6) Mohapatra, S. K.; Misra, M.; Mahajan, V. K.; Raja, K. S. *J. Catal.* **2007**, *246*, 362.

(7) Tachikawa, T.; Tojo, S.; Kawai, K.; Endo, M.; Fujitsuka, M.; Ohno, T.; Nishijima, K.; Miyamoto, Z.; Majima, T. *J. Phys. Chem. B* **2004**, *108*, 19299.

(8) Umebayashi, T.; Yamaki, T.; Itoh, H.; Asai, K. *Appl. Phys. Lett.* **2002**, *81*, 454.

(9) Hong, X. T.; Wang, Z. P.; Cai, W. M.; Lu, F.; Zhang, J.; Yang, Y. Z.; Ma, N.; Liu, Y. *J. Chem. Mater.* **2005**, *17*, 548.

(10) Usseglio, S.; Damin, A.; Scarano, D.; Bordiga, S.; Zecchina, A.; Lamberti, C. *J. Am. Chem. Soc.* **2007**, *129*, 2822.

(11) Hu, C.; Hu, X.; Wang, L. S.; Qu, J. H.; Wang, A. M. *Environ. Sci. Technol.* **2006**, *40*, 7903.

(12) Zhao, J.; Wu, T.; Oikawa, K.; Hidaka, H.; Serpone, N. *Environ. Sci. Technol.* **1999**, *32*, 2394.

(13) (a) Bae, E.; Choi, W.; Park, J.; Shin, H. S.; Kim, S. B.; Lee, J. S. *J. Phys. Chem. B* **2004**, *108*, 14093. (b) Bae, E.; Choi, W. *Environ. Sci. Technol.* **2003**, *37*, 147.

(14) (a) Iliev, V.; Tomova, D. *Catal. Commun.* **2002**, *3*, 287. (b) Shang, J.; Chai, M.; Zhu, Y. *Environ. Sci. Technol.* **2003**, *37*, 4494.

(15) Macyk, W.; Kisch, H. *Chem. Eur. J.* **2001**, *7*, 1862.

(16) Chen, F.; Deng, Z. G.; Li, X. P.; Zhang, J. L.; Zhao, J. C. *Chem. Phys. Lett.* **2005**, *415*, 85.

(17) Li, Y. Z.; Kunitake, T.; Fujikawa, S. *Langmuir* **2007**, *19*, 575.

(18) (a) Pan, J. X.; Xu, Y. H.; Benko1, G.; Feyziyev, Y.; Styring, S.; Sun, L. C.; Akermark, B.; Polivka, T.; Sundstrom, V. *J. Phys. Chem. B* **2004**, *108*, 12904. (b) Kamat, P. V. *J. Phys. Chem.* **1989**, *93*, 859.

(19) Linsebigler, A. L.; Lu, G. Q.; Yates, J. T, Jr *Chem. Rev.* **1995**, *95*, 735–758.

(20) Kamat, P. V. *Chem. Rev.* **1993**, *93*, 267.

(21) Yanagisawa, K.; Ovenstone, J. *J. Phys. Chem. B* **1999**, *103*, 7781.

(22) Li, Y. Z.; Kunitake, T.; Fujikawa, S. *J. Phys. Chem. B* **2006**, *110*, 13000.

(23) Wu, T.; Liu, G.; Zhao, J.; Hidaka, H.; Serpone, N. *J. Phys. Chem. B* **1999**, *103*, 4862.

(24) Li, X. Z.; Liu, G. M.; Zhao, J. C. *New J. Chem.* **1999**, *23*, 1193.

(25) Couselo, N.; Einschlag, F. S. G.; Candal, R. J.; Jobbagy, M. *J. Phys. Chem. C* **2008**, *112*, 1094.

(26) Chen, C. C.; Fan, H. J.; Jang, C. Y.; Jan, J. L.; Lin, H. D.; Lin, C. S. *J. Photochem. Photobiol. A* **2006**, *184*, 147.

JP8055152